Current Applied Physics 20 (2020) 344–351

Contents lists available at ScienceDirect

Current Applied Physics

journal homepage: www.elsevier.com/locate/cap

Superhydrophobic MoS_2-based multifunctional sponge for recovery and detection of spilled oil

Tae-Jun Ko[a], Jae-Hoon Hwang[b], Dwight Davis[c], Mashiyat Sumaiya Shawkat[a,d], Sang Sub Han[a,e], Kelsey L. Rodriguez[b], Kyu Hwan Oh[e], Woo Hyoung Lee[b], Yeonwoong Jung[a,d,f,*]

[a] NanoScience Technology Center, University of Central Florida, Orlando, FL, 32826, USA
[b] Department of Civil, Environmental, and Construction Engineering, University of Central Florida, Orlando, FL, 32816, USA
[c] Department of Mechanical and Aerospace Engineering, University of Central Florida, Orlando, FL, 32816, USA
[d] Department of Electrical and Computer Engineering, University of Central Florida, Orlando, FL, 32816, USA
[e] Department of Materials Science and Engineering, Seoul National University, Seoul, 08826, Republic of Korea
[f] Department of Materials Science and Engineering, University of Central Florida, Orlando, FL, 32816, USA

ARTICLE INFO

Keywords:
Molybdenum disulfide (MoS_2)
Oil-water separation
Oil recovery sponge
Spilled oil recovery
Oil detection

ABSTRACT

Oil spills are a major threat to the marine ecosystem, requiring immediate solutions to remove spilled oil from oceanic environments. In this study, we report a superhydrophobic molybdenum disulfide (MoS_2) coated polydimethylsiloxane (PDMS) sponge and demonstrate its high proficiency in spilled oil recovery and oil spill detection based on oil-water separation ability. This novel oil sorbent is fabricated by a simple dip-coating to incorporate MoS_2 flakes into PDMS sponge. The optimized MoS_2-sponge displays a water contact angle of > 152°, demonstrating excellent superhydrophobicity and high oil absorption (> 97 wt%) for a variety of oils, including vegetable oil and fuel waste. Moreover, the material retains excellent oil absorption capability upon repetitive compression cycles. The versatility of this novel sorbent has been extended for the real-time spontaneous detection of oils by taking advantage of electrically conductive MoS_2 layers.

1. Introduction

Oil spills can occur as a result of various incidents involved in its transportation [1–3] and can be particularly detrimental to marine environments [4–6]. Current methods of oil spill remediation typically fall under three categories; mechanical removal (using sorbents, skimming), in-situ burning, and usage of chemical dispersants [7,8]. Amongst them, direct burning and usage of chemical dispersants are a highly effective method in responding to a wide range of oil spills, but it often produces secondary pollution [9–12]. Despite the environmental benignity, the mechanical removal approach suffers from low separation efficiency of spilled oil from contaminated water. So, development of absorbent materials which can efficiently select oil in a non-chemical manner should be pursued [13], which incorporates the following aspects: 1) high hydrophobicity and oleophilicity for oil-water selectivity, 2) a highly porous structure for increased oil absorption capacity, 3) high mechanical stability for repeated use, and 4) low production cost. Over the past decades, a variety of oil-absorbing natural materials with intrinsic structural porosity have been proposed [15–17]. Simultaneously, substantial efforts have been made to develop oil-absorbing functional materials such as polypropylene and aerogels via chemical routes to achieve lower production cost and improved hydrophobicity [18–20]. To this end, a variety of nano-engineering approaches have been employed, including surface modification and coating techniques [14,21–26]; for instance, various oil-absorbing sponges coated with functional nanomaterials such as magnetite (Fe_3O_4), titanium dioxide (TiO_2) nanoparticles, graphdiyne, and graphene were reported [27–31]. Furthermore, a graphene-based sponge with high thermal conductivity was explored, and its intrinsic Joule heating was utilized for enhancing oil removal efficiency [32]. As a new functional nanomaterial to achieve the desired hydrophobicity, two-dimensional (2D) transition metal dichalcogenides (TMDs) have attracted lots of attention due to their intrinsically layered crystallinity which can be tailored toward optimized properties. Particularly, 2D molybdenum disulfide (MoS_2) layers possess a wide range of intrinsic hydrophobicity varying with their layer orientation [33] as well as tunable surface energy that varies upon exposure to airborne moisture and hydrocarbon contamination [34]. Previous studies have reported that 2D MoS_2 layers-coated oil sorbents have a superior oil-water separation by utilizing superhydrophobicity (water contact angle > 150°) and superoleophilicity

* Corresponding author. 12424 Research Parkway, Orlando, FL, 32826, USA.
E-mail address: yeonwoong.jung@ucf.edu (Y. Jung).

https://doi.org/10.1016/j.cap.2019.12.001
Received 2 August 2019; Received in revised form 8 November 2019; Accepted 2 December 2019
Available online 03 December 2019
1567-1739/ Published by Elsevier B.V. on behalf of Korean Physical Society.

(oil contact angle < 10°) [35,36]. While these successful demonstrations benefit from the structural uniqueness of 2D MoS_2 layers, further studies on the modification of fabrication procedures for simple sponge preparation, improvement of hydrophobicity, and expanded tests with various oily wastes are required to advance the technology into effective operational responses for oil spill events. In addition, their other excellent properties such as high electrical conductivity have never been utilized [37]. Therefore, their full potential for further advanced oil spill management has remained largely unexplored.

Herein, we developed the oil spill managing MoS_2-coated PDMS sponge (MoS_2-sponge) with superior multifunctionality by incorporating hydrophobic 2D MoS_2 layers into a structurally engineered PDMS of high porosity and oleophilicity. PDMS, which is a widely used silicone-based elastic polymer due to non-toxic, inert, and highly elastic properties, was employed as a template to achieve the targeted porosity, while MoS_2 layers were incorporated via a simple solution process [28,38,39]. Also, the PDMS presents excellent mechanical elasticity and resilience, which are essential considerations to achieve the desired reusability of the sponges upon their repeated squeezing/relaxing for oil absorption/extraction. Amongst various template methods to fabricate porous structures in PDMS sponges [38,40–44], sugar cubes offer a distinguishable advantage of having a low cost, environmental benignity, and simple fabrication [39]. The MoS_2-sponge exhibit highly-efficient selective absorption and recovery of oil with a simultaneous repulsion of water as well as high recyclability. Moreover, the high intrinsic electrical conductivity of MoS_2 layers allows for real-time in-situ detection of oil penetration kinetics, greatly broadening the versatility of the sponges for advanced oil spill remediation applications.

2. Materials and methods

2.1. Fabrication of PDMS sponges

Porous PDMS sponges were fabricated using commercially available cube sugars as a template material in the following process; elastomer (Dow Corning Sylgard 184 A) and curing agent (Dow Corning Sylgard 184 B) were mixed at a mass ratio of 10:1, followed by the mixture being poured into a sugar cube template ($1 \times 1 \times 1$ cm^3). Then, the mixture of the solution with the sugar was placed on a hotplate and cured at 80 °C for 2 h, which results in elastic PDMS. The prepared PDMS/sugar composite was immersed in deionized (DI) water under ultrasonication with 40 kHz at 70 °C for 2 h to dissolve the sugar particles. Upon dissolution of the sugar particles, the PDMS was taken out from the water bath and allowed for natural drying yielding a porous PDMS sponge.

2.2. MoS_2 flakes coating on the PDMS sponge

MoS_2 flakes, which are stacks of the 2D layered structure, were coated on PDMS sponges *via* a dip-drying method. Commercially available MoS_2 flakes (CAS No. 1317-33-5, super-fine grade, > 99%, Climax Molybdenum, AZ, USA) were dispersed in isopropyl alcohol (IPA) solution followed by sonication. The separately prepared PDMS sponge was dipped into the IPA solution containing the MoS_2 flakes with designated mixing ratios of IPA:MoS_2 (from 200:1 to 25:1) and was ultrasonicated for 2 h with 40 kHz. Subsequently, the PDMS/MoS_2 composite was heated up to 70 °C to evaporate IPA, which ensures the direct/robust attachment of MoS_2 flakes to the PDMS surface.

2.3. Material characterization of MoS_2-sponges

The porous structures of the MoS_2-sponge were observed using an optical microscope (BX60M, Olympus, Japan) and a scanning electron microscope (SEM, Nova NanoSEM 200, FEI, USA) at a 5 kV electron accelerating voltage. Also, energy-dispersive X-ray spectroscopy (EDS, Apollo X, EDAX Inc., USA) was utilized to analyze the chemical composition change before and after coating MoS_2 flakes. The hydrophobicity of the MoS_2-sponge was identified by measuring the water contact angle (CA) of DI water through a sessile drop test. 4 μL of water droplets were gently deposited on the MoS_2-sponge surface using a microsyringe, and the CA was measured by a goniometer (Model 90, Rame-Hart, USA) in ambient air at room temperature under 20–35% of relative humidity. The CA was determined from at least four different spots in each sample, and the average value was calculated. The mechanical property of MoS_2-sponge was measured using a universal testing machine (MTS Exceed E42, MTS Systems Corporation, USA) equipped with 500 N load cell. A cuboid-shaped MoS_2-sponge with a size of $6 \times 6 \times 10$ mm^3 was placed between two flat stages designed for compression test. Compression and release rates were set to 0.2 mm/s. The compressive and release behaviors were recorded with digital camera (EOS 60D, Canon Inc., Japan).

2.4. Oil absorption and recovery tests

A variety of oils and organic solvents, including shipboard standard bilge mix (SBM), canola oil, toluene, hexane, and polyethylene glycol, were utilized to evaluate the oil absorption and recovery performance of the MoS_2-sponge. Transparent organic solvents such as hexane, toluene, and polyethylene glycol were dyed with Sudan IV (dye content ≥ 80%, Sigma-Aldrich, USA) for improved visualization of oil absorption. For absorption capacity measurements, a MoS_2-sponge of $1 \times 1 \times 1$ cm^3 in volume and the oil/organic solvent of 10 mL were used. The kinetics of oil absorption were identified by measuring the weight of the oil absorbed by the MoS_2-sponge (wt%) as a function of absorption duration. The recyclability of the MoS_2-sponge in repeatedly absorbing and releasing oil was tested by manually squeezing the oil-absorbed MoS_2-sponge, which was subsequently dried for 10 min. The completely dried MoS_2-sponge was reused to absorb the oil/organic solvent up to 8 cycles. For a continuous oil collection test, an oil-absorbed MoS_2-sponge connected to a peristaltic liquid pump (12 V DC dosing pump, Gikfun, China) by a Teflon tube was placed in a beaker containing water and hexane mixture. The pumping rate was maintained to 1.15 mL/s for 4 h. The pumping flux was obtained by measuring the oil collection rate of every 15 min. Following each measurement, the collected oil was recycled back to the starting point so that the initial volume of liquid remained constant.

2.5. Electrical measurement

The electrical characterization of the MoS_2-sponge for a real-time oil detection was carried out using a semiconductor parameter analyzer (HP 4156A, Hewlett-Packard, USA) connected to a home-built probe station. Conductance values were extracted by the linear fitting of the current-voltage (I–V) plots (Conductance (G) = 1/Resistance (R)) at a voltage range from −5.0 to 5.0 V. The kinetics of oil absorption into the MoS_2-sponge was manifested by monitoring the variation of current as a function of time.

3. Results and discussion

3.1. Morphology & element analysis of MoS_2-sponge

The fabrication procedure of MoS_2-sponge using a sugar cube template is illustrated in Fig. 1a. The sugar cube constitutes of individual sugar particles of about 100 μm was employed as a template replicating a PDMS sponge of corresponding porosity, as shown in Fig. 1b. Then, commercially available MoS_2 flakes of about 1 μm in size (Fig. 1c) were incorporated on the surface and interior of the PDMS sponge by a dip-drying method; MoS_2 flakes dispersed in IPA were directly injected into the sponge where IPA efficiently prevents their van der Waals attraction-driven agglomeration owing to its low surface energy [45].

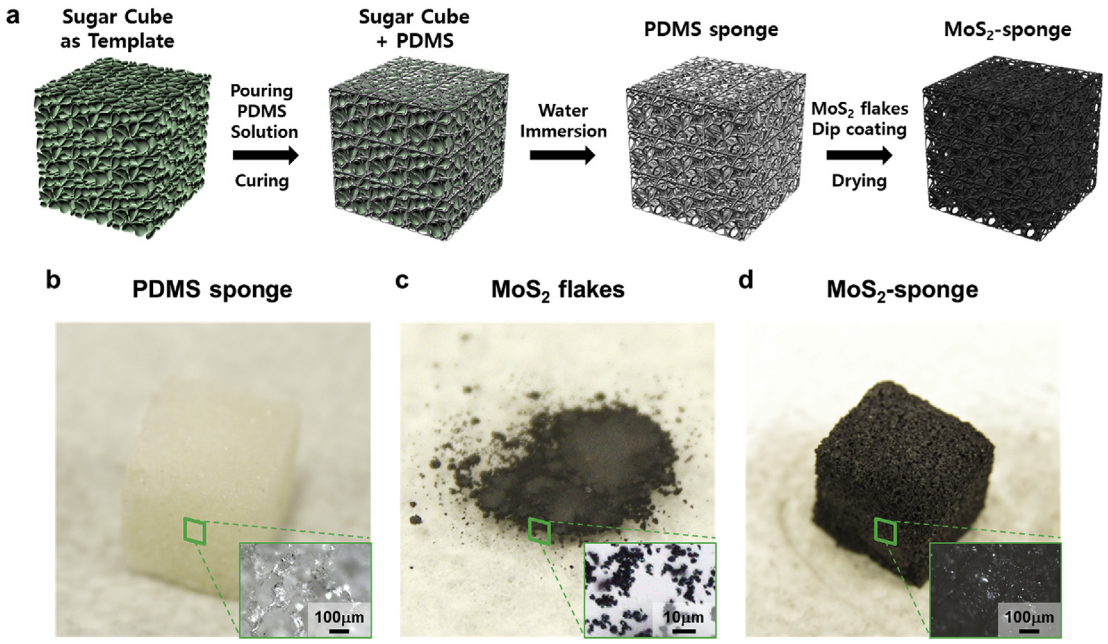

Fig. 1. (a) Fabrication process of MoS_2-sponge. (b–d) Photo images of (b) a PDMS sponge, (c) MoS_2 flakes, and (d) a MoS_2-sponge, respectively. The insets show the optical microscopy images of the corresponding photo images.

Heating and ultrasonication were also applied in dispersing MoS_2 flakes in IPA to further improve their spatial homogeneity throughout the entire PDMS sponge [36,46]. As shown in Fig. 1d, the color of the sponge becomes darker with increasing the concentration of MoS_2 flakes.

The morphological and chemical integrity of PDMS sponges throughout their fabrication process and MoS_2 flakes incorporation were identified using SEM and EDS. As-prepared PDMS sponges in their pristine form are highly porous, constituting a large density of pores of various sizes (Fig. 2a) while their exposed surfaces are highly smooth (Fig. 2b). MoS_2 flakes were separately prepared by ultrasonication (Fig. 2c) and incorporated into the PDMS sponges without altering their intrinsic porosity (Fig. 2d). Note that dimension of individual 2D MoS_2 flakes (typically $<$ 1 μm) is much smaller than that of PDMS pores (typically in a range of ~10 μm to 1 mm). Upon incorporation of MoS_2 flakes, the PDMS surface turns rough owing to their exposure on it, as shown in Fig. 2e. The chemical composition of the MoS_2-sponge was characterized by EDS to examine the spatial distribution of constituent elements. Fig. 2f shows EDS secondary electron image and elemental mapping image revealing their distributions, i.e., Mo, S from MoS_2 flakes, and Si from PDMS. The SEM images and EDS mapping images confirm that MoS_2 flakes are homogeneously dispersed and attached on the surface of PDMS via strong van der Waals force. Moreover, Mo and S signals were localized within PDMS undetected in the porous regions,

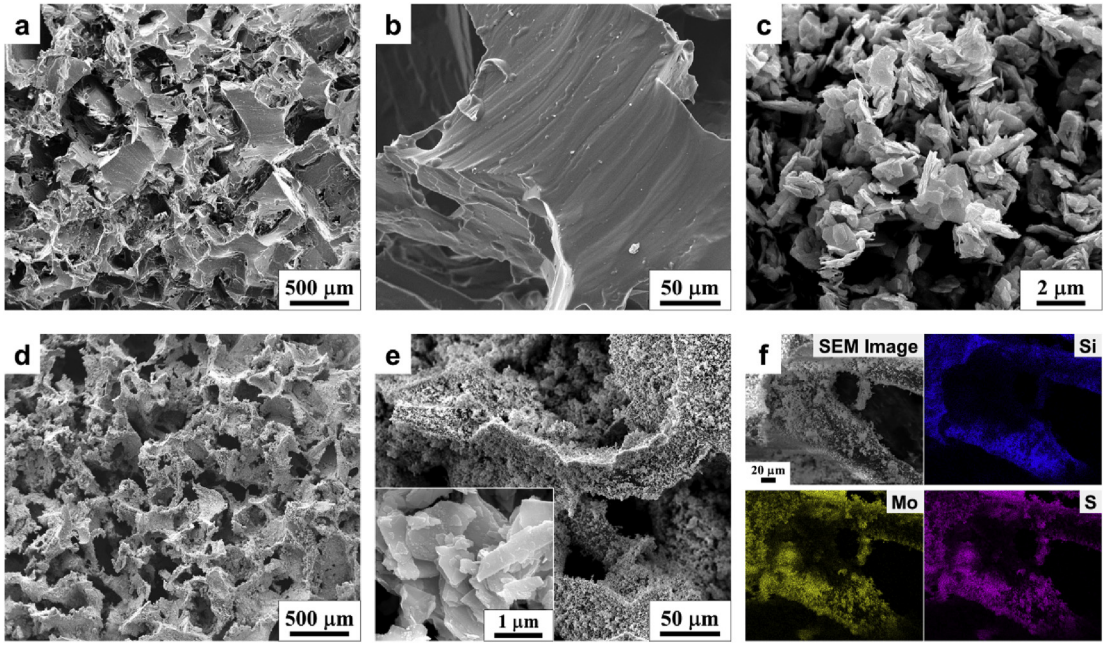

Fig. 2. (a–c) SEM images showing (a) porosity of a PDMS sponge at low magnification, (b) surface smoothness of the sponge, (c) morphology of MoS_2 flakes. (d) SEM image of a MoS_2-sponge at the magnification identical to (a). (e) SEM image showing the hierarchical surface roughness of the sponge after MoS_2 coating. (f) SEM image and EDS elemental mapping images of the MoS_2-sponge surface presenting its constituent elements of Si (from PDMS), Mo, and S (from MoS_2 flake).

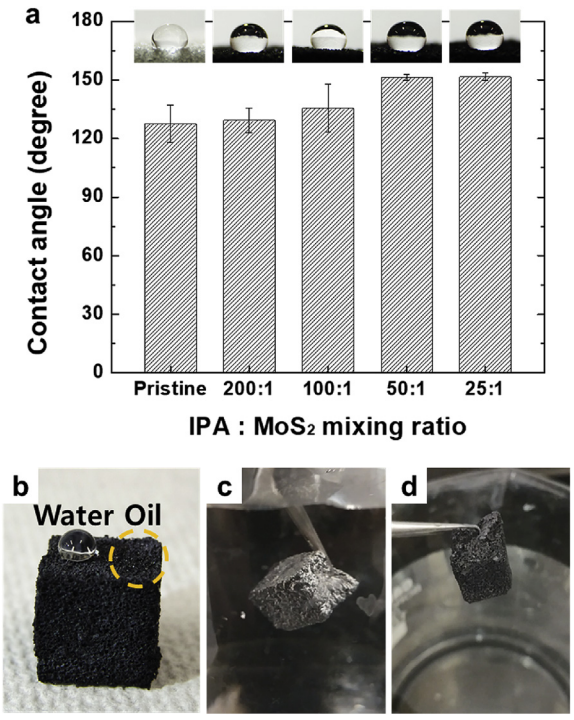

Fig. 3. (a) Water contact angle measurements of MoS_2-sponges prepared with different mixing ratios of IPA:MoS_2. (b) Demonstration of oil absorption and water repulsion. (c) Formation of underwater air-pocket evidencing the repulsion of water. (d) No observation of water on the MoS_2-sponge surface after immersion into the water.

indicating the intrinsic porosity of PDMS was not altered throughout the dip-drying process.

3.2. Wettability of MoS_2-sponge

We investigated the water wettability of MoS_2-sponges responsible for selective oil absorption and optimized it for highly efficient oil spill recovery. PDMS itself is known to be hydrophobic in its pristine state with no porosity and exhibit an intrinsic water contact angle of 108° and surface tension of 23.9 mN/m [47]. This intrinsic hydrophobicity can be drastically increased by incorporating MoS_2 flakes, as below verified; We adjusted the mixing ratio of IPA:MoS_2 and measured resulting water contact angles (CAs) in order to determine the optimum concentration of MoS_2 flakes. If the MoS_2 flakes concentration is too low, they would not entirely cover the surface of the PDMS porous sponge undermining hydrophobicity. If the concentration is too high, the pores will clog, leading to a decrease in oil absorption capacity (see Fig. S1 in Supporting Information). Fig. 3a shows the water CAs of MoS_2-sponges as a function of the mixing ratio of IPA: MoS_2, revealing their increase with an increasing concentration of MoS_2 flakes, e.g., as the mixing ratio changes from 200:1 to 100:1, the CA value increases from 129.3° to 135.5°. With a further increase in the mixing ratio from 50:1 to 25:1, the CA value slightly increases from 151.3° to 151.6°, achieving the desired superhydrophobicity. Having confirmed the superhydrophobicity of MoS_2-sponges, we then investigated their selective oil absorption ability or superoleophilicity. As shown in Fig. 3b, the water droplet prepared with the 50:1 mixing deposited to the sponge surface retained its spherical shape without being absorbed owing to excellent superhydrophobicity. Such superhydrophobicity was well maintained even when the MoS_2-sponge was completely immersed in water, as shown in Fig. 3c. Upon water immersion, the MoS_2-sponge surface instantly and uniformly turns glossy, which is due to the formation of air pockets - numerous pores or cavities containing air. The MoS_2-sponge exhibited no visible sign of wetting once taken out of the water, indicating that it in the Cassie-Baxter state which is a regime of superhydrophobic water wetting [48]. The air pockets formed in the pores effectively repel penetrating water while keeping them dry, as shown in Fig. 3d. Meanwhile, when an oil droplet was deposited to the MoS_2-sponge surface (e.g., olive oil in Fig. 3b), it was instantly and entirely absorbed into the interior of the MoS_2-sponge.

3.3. Oil recovery capacity & efficiency

Various oils and organic solvents which are widely used in worldwide were tested, including petroleum products, hydrocarbon solvents, and vegetable oil. The oil absorption efficiency was quantified by calculating the weight gain (wt%), which is defined as the weight ratio of a

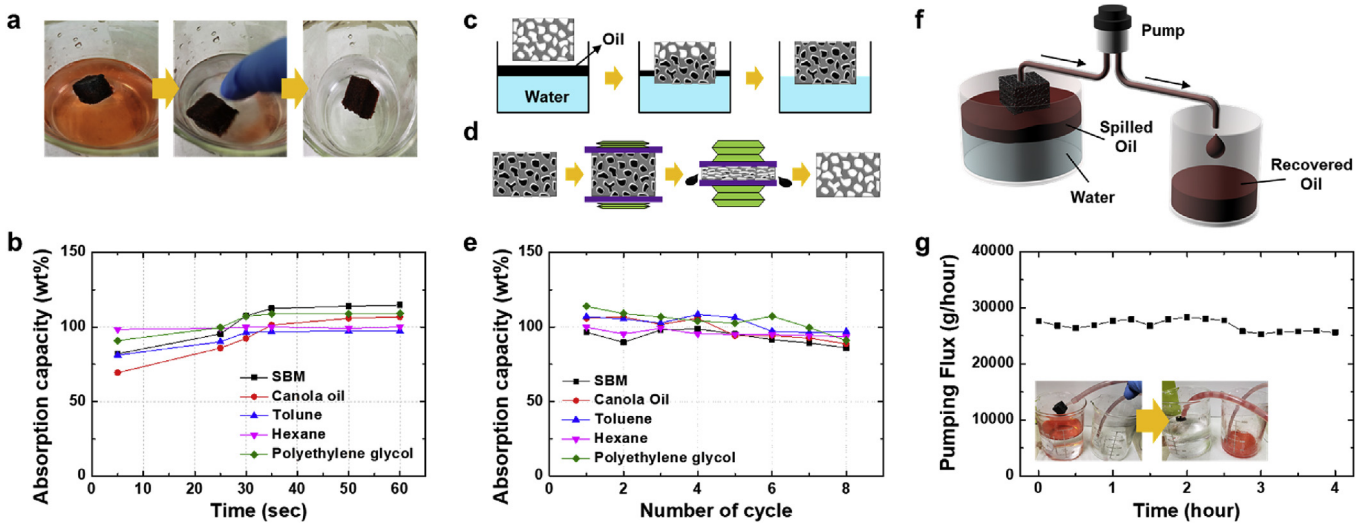

Fig. 4. (a) Sequential images demonstrating the oil collection process from water containing spilled oil - SBM dyed with Sudan IV red. (b) Plots of absorption kinetics for a variety of tested oils with respect to absorption duration. (c, d) Schematics to illustrate; (c) absorption of spilled oil, and (d) desorption of the collected oil by manual squeezing/releasing. (e) Plots of absorption capacity and recyclability for a variety of tested oils. (f) Schematic of the experimental apparatus for the continuous collection of oil from the surface of the water into the recovery vessel. (g) Prolonged stable operation of continuous collection and recovery of oil. The insets show the demonstration image of continuous collection of hexane for 4 h from the water with the pumping apparatus. (For interpretation of the references to color in this figure legend, the reader is referred to the Web version of this article.)

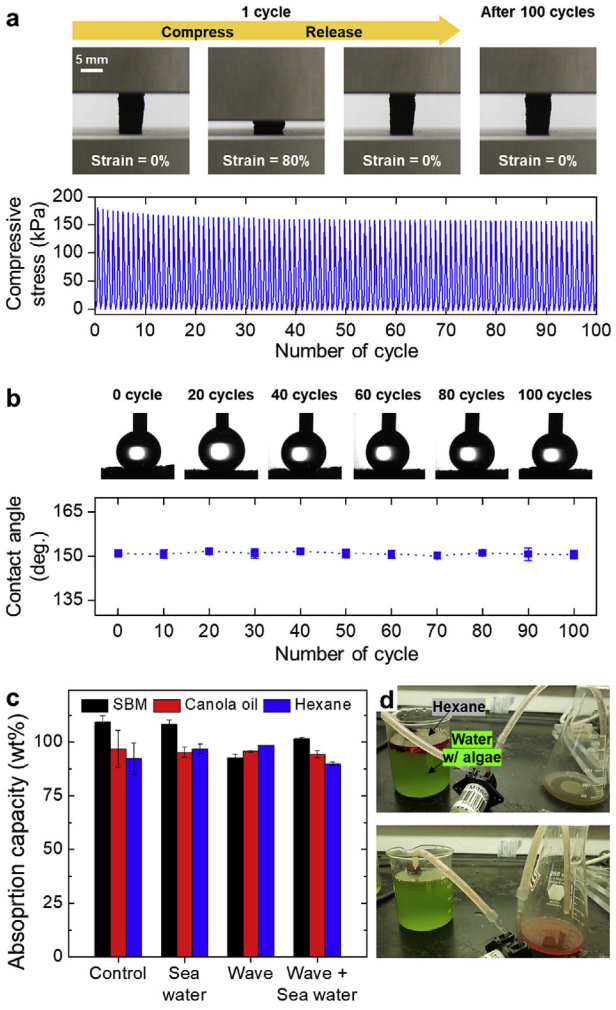

Fig. 5. (a) (top) Sequential photos showing the MoS_2-sponge deformation during a cyclic compression test. (bottom) The compressive stress curve of MoS_2-sponge under 80% of compressive strain for 100 cycles. (b) (top) Sequential photos showing the water contact angle after multiple times of compression test. (bottom) The water CA of MoS_2-sponge during the cyclic compression test. (c) Oil absorption capacity demonstrated in various harsh conditions simulating the real sea environment. (d) Photos of demonstrating the recovery of hexane from algae-containing water using the pumping apparatus.

MoS_2-sponge before/after oil absorption at a given time. As shown in Fig. 4a, once a piece of MoS_2-sponge ($1cm^3$) was dropped into water containing a layer of canola oil (dyed with Sudan IV), it rapidly absorbed the oil only leaving clean water behind within a few seconds. The oil-soaked MoS_2-sponge was removed from each test baths at specific times, and the oil absorption capacity (K) was determined by the difference between the initial weight of the MoS_2-sponge (W_0) and oil-soaked state (W_t) divided by the initial weight (W_0) of the MoS_2-sponge, multiplied by 100;

$$K(\%) = \frac{(W_t - W_0)}{W_0} \times 100$$

The oil absorption kinetics for a variety of tested oils as a function of oil absorption time is presented in Fig. 4b. Within 60 s of absorption, the MoS_2-sponges exhibited high absorption efficiencies for all the tested oils including SBM, canola oil, and chemicals (toluene, hexane, polyethylene glycol) as manifested by K of ~97.3–114.6 wt%. It took less than 5 s to reach an equilibrium state absorbing hexane which possesses the lowest viscosity (0.3 mPa s at 25 °C). Meanwhile, at least 50 s were required to fully absorb highly viscous oils such as canola oil (46.2 mPa s at 30 °C) owing to the high shear force needed for their penetration into the pores inside the MoS_2-sponge [49,50].

To further test the repeatability of MoS_2-sponges for prolonged oil-spill management, we investigated their oil absorption capacity change for repeated oil absorption/desorption. Upon full oil saturation, the MoS_2-sponges were mechanically squeezed desorbing the collected oils, as shown in Fig. 4c and d. Due to their elastic nature (Fig. S2), the MoS_2-sponges fully recover their initial forms upon releasing the oil and are ready for subsequent oil absorption. Fig. 4e shows the repeatable use of the MoS_2-sponges for absorbing various types of oils. After eight cycles of absorption/desorption, the absorption capability was observed to slight decrease (average: 12.7 ± 5.5%), which is possibly due to some residual oil, which was not entirely come out by squeezing during each cycle. This observed repeatability, i.e., absorption capability given the identical cycle number is superior to the performance of previously developed sponges such as copper nanoparticles-coated sponges or graphite-based sponges, which drastically deteriorated after two cycles [51,52].

To demonstrate the continuous collection of oil from a water surface with a lab-scale simulated oil spill event, we have prepared a batch-scale pumping apparatus, as shown in Fig. 4f (Movie S1). It is known that collecting spilled oil by pumping through a porous sorbent in a continuous manner can greatly simplify the oil recovery process and reduce materials consumption [23,32]. In the initial pumping test, 15 mL of hexane was collected from the oil-water mixture, and no water was found in the collection tank (shown in the insets of Fig. 4g), demonstrating high oil-water separation ability and spilled oil recovery efficiency. The long-term continuity of oil extraction under a constant supply of oil has been demonstrated for 4 h (Movie S2), achieving full recovery of hexane from oil-water mixture without significant degradation of recovery efficiency, as shown in Fig. 4g. Notably, the optimized balance of capillary pressure and suction power prevents the penetration of water and air into the pores in the MoS_2-sponge, and only the oil is absorbed into the MoS_2-sponge and flows through the tube to the collection tank, allowing the MoS_2-sponge can uptake the supplied oil persistently [23].

Supplementary data related to this article can be found at https://doi.org/10.1016/j.cap.2019.12.001.

We also investigated the mechanical properties of the MoS_2-sponge with a cyclic compression test. Recently, as the awareness that the disposal of used oil sorbents can cause secondary environmental pollution is spreads, the importance of reusability and recyclability of oil sorbents has been increasing. However, it is known that the mechanical compression for recovery of absorbed oil through the squeezing can destroy internal fiber-based porous structures, as a result of which the oil absorption capacity is significantly reduced. As an example, conventional oil sorbents made from natural or synthetic fibers such as polypropylene fibers exhibit very low reusability of fewer than 10 times [53]. In order to utilize the oil sorbent multiple times, the sorbent material requires high mechanical resilience during the physical squeezing in the oil recovery process. With this in mind, we tested the cyclic resilience by measuring the compressive stress of the MoS_2-sponge [54]. Fig. 5a shows the MoS_2-sponge during the cyclic compression test at 80% strain for 100 cycles. It was found that the shape and the volume of MoS_2-sponge fully recover even after 100 cycles of compression, which indicates that the MoS_2-sponge has high mechanical resilience under compression. The bottom graph in Fig. 5a exhibits the compressive stress value of the MoS_2-sponge during the cyclic compression test. The compressive stress almost linearly decreased by 8.8% with increasing of the number of cycles during 20 cycles of compression, and the value further decreased by 11.4% after 40 cycles of compression. With further compression cycles, the reduction of the compressive stress has been saturated, maintaining 13.8% reduction after 100 cycles. This reduction tendency is supposed to be induced by breakage of a few skeletons inside of the sponge at the initial stage of compression cycles. But the internal pore structures were well preserved due to high elasticity of PDMS (base material), therefore, the

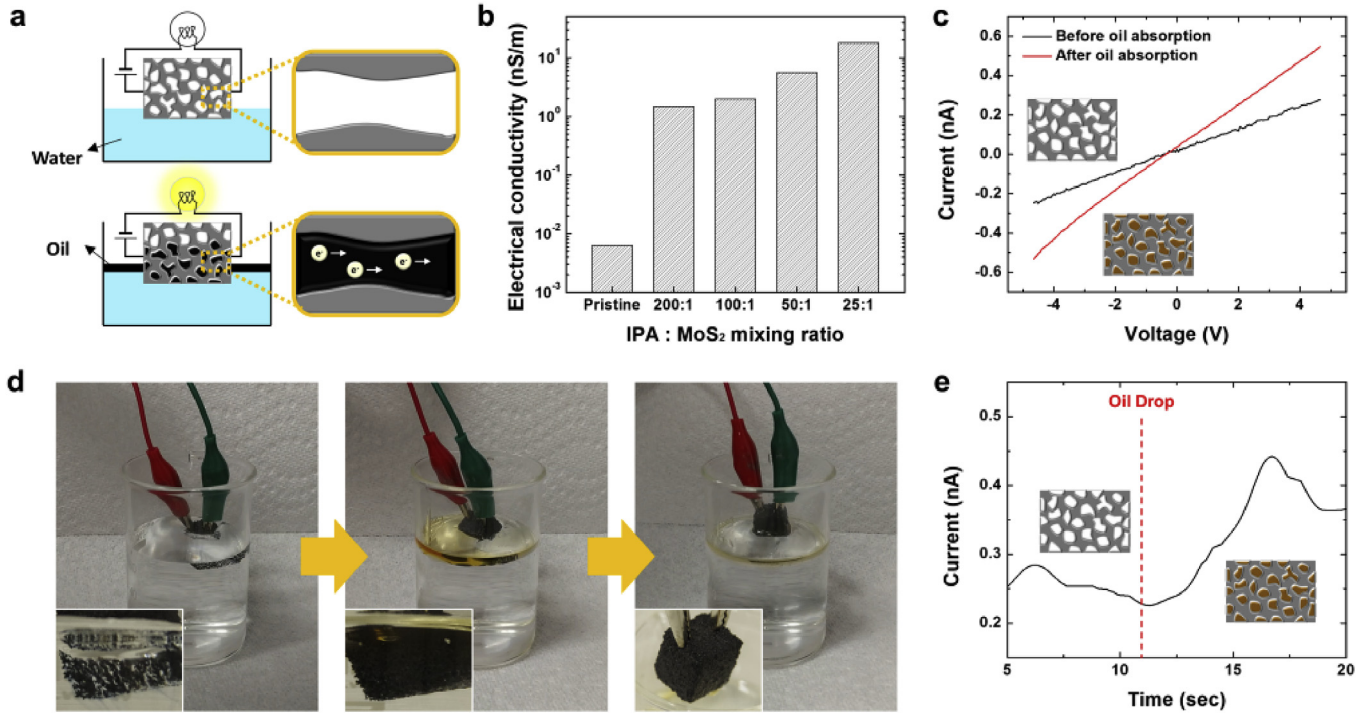

Fig. 6. (a) Schematics to illustrate the electrical detection of conductive oil. (b) Electrical conductance measurement of MoS_2-sponges prepared with varying mixing ratios of IPA:MoS_2. (c) I–V characteristics from a MoS_2-sponge before and after oil absorption. (d,e) Real-time electrical detection of SBM; (d) Sequential images to show the electrical oil monitoring process, and (e) Current change following by the oil absorption which is shown in (d).

MoS_2-sponge shows high resiliency against multiple cycles of compression. Additionally, the water CA during the cyclic compression tests is also evaluated, which is essential to render robust oil-water separation. As shown in Fig. 5b, the water CA remained above 150° during the 100 cycles of compression, indicating the oil-water separation ability based on superhydrophobicity is also well maintained. Overall, the MoS_2-sponge displays high reusability due to its durability and robustness.

We also studied the oil absorption capability of the MoS_2-sponge in a harsh condition by simulating an actual sea environment in terms of salinity and turbulence. For that, we prepared for brine (3.5% NaCl) and simulated waves in it using a stirrer to examine the effect of salinity and external pressure, respectively. The oil recovery test was carried out for 50 s under the brine condition with and without the simulated waves and the resulting recovery capabilities were compared. As shown in Fig. 5c, the oil absorption capacities of the MoS_2-sponge showed no decrease regardless of the brine conditions, indicating its reliable operation even under high salinity and turbulence. It is noted that the MoS_2-sponge floats well on the water surface even under agitation due to its low density and high buoyancy. Additionally, the continuous oil recovery capability of the MoS_2-sponge was tested with algae-containing water using the pumping apparatus. As shown in Fig. 5d, only hexane was absorbed into the MoS_2-sponge and the absorbed hexane was fully recovered by being transported to a secondary container through the tube connected to the pump. This result presents that water even in its algae-containing state becomes efficiently repelled from the MoS_2-sponge due to its excellent superhydrophobicity.

3.4. Real-time electrical detection of spilled oil

After the successful development of high-efficiency oil clean-up using MoS_2-sponge in their pristine form, we extend their versatility for the electrical detection of spilled oil and the real-time monitoring of oil absorption kinetics. We propose a new type of oil-detecting platform which benefits from the intrinsic oil-water separation ability of the MoS_2-sponge as well as its electrical conductivity resulting from the incorporated MoS_2. This device is particularly more functional for detecting oils of intrinsic electrical conductivity – *e.g.*, SBM, crude oil. Fig. 6a illustrates the proposed concept comparing two situations of; (top) before oil absorption, (bottom) after oil absorption. The MoS_2-sponge floating on DI water without any oil absorption (top) exhibits a low electrical response. However, when it becomes saturated with conductive oils (bottom), it exhibits an increase of electrical conductance as the conductive components in the oil fill in the pores within it. It is known that the conductivity of air and the crude oil are about 3–8 pS/m and 10–45 nS/m at room temperature, respectively [55]. In addition, the conductivity of SBM used in our demonstration was measured at 24.4 ± 3.7 nS/m, which was comparable to that of crude oil. When the MoS_2-sponge contacts with oil, it spontaneously absorbs the oil, which easily penetrates through its porous channels, thus electrical conductance increases. Before the actual demonstration of electrical sensing, we first characterized the electrical conductivity of MoS_2-sponges prepared with varying IPA:MoS_2 mixing ratios. As shown in Fig. 6b, the electrical conductivity significantly increases with increasing the concentration of MoS_2 flakes. The conductivity of a pristine PDMS sponge without incorporating MoS_2 flakes was 6.3 pS/m, and it increases to 1.5 nS/m after incorporating them with IPA:MoS_2 = 200:1. With the mixing ratio of 50:1 and 25:1, the conductivity further increases to 5.6 and 18 nS/m, respectively, corresponding to ~1000 times than that of the bare PDMS. Fig. 6c shows the current-voltage (I–V) characteristics of a MoS_2-sponge prepared with 50:1 mixing ratio before and after oil absorption. As above predicted, upon absorbing the oil (SBM, in this case), the current value increases nearly two times in the tested range of −4 V to 4 V; e.g., 0.24 nA increases to 0.47 nA at 4 V. Based on this confirmation, the proof-of-concept demonstration of real-time oil detection was achieved by monitoring the current change with respect to time at a constant voltage of 4 V as shown in Fig. 6d and e. When the MoS_2-sponge was initially in contact with water only, no significant current change was detected indicating there was no absorption of water due to its superhydrophobicity. However, upon

dripping the oil to the water (at 11 s in Fig. 6e), a drastic increase of current was observed, indicating its significant absorption. As shown in the first image of Fig. 6d, the MoS_2-sponge was initially covered with air-pockets due to its superhydrophobicity when it was only in contact with water, resulting in a no electrical response. However, once the MoS_2-sponge was exposed to the oil, the air-pockets instantly disappeared and were replaced with it forming various pathways for the transport of charged particles within the MoS_2-sponge. The schematics in the insets of Fig. 6c and e illustrate this distinction.

4. Conclusion

In this study, we developed multifunctional MoS_2-sponges and demonstrated their rapid and efficient recovery and detection of spilled oil in water. This novel oil absorbent material realized by the simple template-replicated fabrication of porous PDMS sponges and the incorporation of MoS_2 flakes by a dip-coating method exhibits essential attributes to selective oil absorption and water repulsion. The MoS_2-sponge exhibits excellent superhydrophobicity (water CA $>$ 152°) and high oil absorption ($>$ 97 wt%) through the tests with a variety of oils, including vegetable oil and fuel waste such as SBM. Also, the material can be recycled more than eight times preserving its excellent oil absorption capacity upon a repetitive absorption/desorption of the oils enabled by its elastic deformation. The versatility of this sorbent material has been further extended for the real-time electrical detection of conductive oil in a simulated situation. The study suggests a massive technological implication of this new sorbent material for managing oil spill incidents in real-world situations.

Declaration of competing interest

The authors declare that they have no known competing financial interests or personal relationships that could have appeared to influence the work reported in this paper.

Acknowledgment

This project was supported by the US Environmental Protection Agency as EPA P3 program I (grant No. SU839263) and II (grant No. SU839489). This work was also supported by NSF I-Corps (project number 1935619).

Appendix A. Supplementary data

Supplementary data to this article can be found online at https://doi.org/10.1016/j.cap.2019.12.001.

References

[1] W. Zhang, Y. Zhu, X. Liu, D. Wang, J. Li, L. Jiang, J. Jin, Salt-induced fabrication of superhydrophilic and underwater superoleophobic PAA-g-PVDF membranes for effective separation of oil-in-water emulsions, Angew. Chem. 53 (2014) 856–860.
[2] P. Burgherr, In-depth analysis of accidental oil spills from tankers in the context of global spill trends from all sources, J. Hazard Mater. 140 (2007) 245–256.
[3] A. Jernelöv, The threats from oil spills: now, then, and in the future, Ambio 39 (2010) 353–366.
[4] A.C. Bejarano, J. Michel, Oil spills and their impacts on sand beach invertebrate communities: a literature review, Environ. Pollut. 218 (2016) 709–722.
[5] J. Beyer, H.C. Trannum, T. Bakke, P.V. Hodson, T.K. Collier, Environmental effects of the Deepwater Horizon oil spill: a review, Mar. Pollut. Bull. 110 (2016) 28–51.
[6] Ø. Langangen, E. Olsen, L.C. Stige, J. Ohlberger, N.A. Yaragina, F.B. Vikebø, B. Bogstad, N.C. Stenseth, D.Ø. Hjermann, The effects of oil spills on marine fish: implications of spatial variation in natural mortality, Mar. Pollut. Bull. 119 (2017) 102–109.
[7] I.B. Ivshina, M.S. Kuyukina, A.V. Krivoruchko, A.A. Elkin, S.O. Makarov, C.J. Cunningham, T.A. Peshkur, R.M. Atlas, J.C. Philp, Oil spill problems and sustainable response strategies through new technologies, Environ. Sci.: Process. Impacts 17 (2015) 1201–1219.
[8] J. Ge, H.-Y. Zhao, H.-W. Zhu, J. Huang, L.-A. Shi, S.-H. Yu, Advanced sorbents for oil-spill cleanup: recent advances and future perspectives, Adv. Mater. 28 (2016) 10459–10490.
[9] A.C. Bejarano, Critical review and analysis of aquatic toxicity data on oil spill dispersants, Environ. Toxicol. Chem. 37 (2018) 2989–3001.
[10] S. Kleindienst, J.H. Paul, S.B. Joye, Using dispersants after oil spills: impacts on the composition and activity of microbial communities, Nat. Rev. Microbiol. 13 (2015) 388.
[11] R.C. Prince, Oil spill dispersants: boon or bane? Environ. Sci. Technol. 49 (2015) 6376–6384.
[12] S. Rahsepar, M.P.J. Smit, A.J. Murk, H.H.M. Rijnaarts, A.A.M. Langenhoff, Chemical dispersants: oil biodegradation friend or foe? Mar. Pollut. Bull. 108 (2016) 113–119.
[13] M. Ha, H.-K. Cheong, Oil spill clean-up: a trade-off between human health and ecological restoration? Lancet Publ. Health 2 (2017) e534–e535.
[14] S. Woo, W. Kwak, W. Hwang, Sequential liquid separation using meshes with hierarchical microcube–nanohole structure and controlled surface wettability, Appl. Surf. Sci. 462 (2018) 237–242.
[15] M.O. Adebajo, R.L. Frost, J.T. Kloprogge, O. Carmody, S. Kokot, Porous materials for oil spill cleanup: a review of synthesis and absorbing properties, J. Porous Mater. 10 (2003) 159–170.
[16] G. Deschamps, H. Caruel, M.-E. Borredon, C. Bonnin, C. Vignoles, Oil removal from water by selective sorption on hydrophobic cotton fibers. 1. Study of sorption properties and comparison with other cotton fiber-based sorbents, Environ. Sci. Technol. 37 (2003) 1013–1015.
[17] A. Bayat, S.F. Aghamiri, A. Moheb, G.R. Vakili-Nezhaad, Oil spill cleanup from sea water by sorbent materials, Chem. Eng. Technol. 28 (2005) 1525–1528.
[18] C. Teas, S. Kalligeros, F. Zanikos, S. Stournas, E. Lois, G. Anastopoulos, Investigation of the effectiveness of absorbent materials in oil spills clean up, Desalination 140 (2001) 259–264.
[19] G. Wang, H. Uyama, Facile synthesis of flexible macroporous polypropylene sponges for separation of oil and water, Sci. Rep. 6 (2016) 21265.
[20] Q.F. Wei, R.R. Mather, A.F. Fotheringham, R.D. Yang, Evaluation of nonwoven polypropylene oil sorbents in marine oil-spill recovery, Mar. Pollut. Bull. 46 (2003) 780–783.
[21] O. Oribayo, X. Feng, G.L. Rempel, Q. Pan, Modification of formaldehyde-melamine-sodium bisulfite copolymer foam and its application as effective sorbents for clean up of oil spills, Chem. Eng. Sci. 160 (2017) 384–395.
[22] J. Pinto, A. Athanassiou, D. Fragouli, Surface modification of polymeric foams for oil spills remediation, J. Environ. Manag. 206 (2018) 872–889.
[23] J. Ge, Y.-D. Ye, H.-B. Yao, X. Zhu, X. Wang, L. Wu, J.-L. Wang, H. Ding, N. Yong, L.-H. He, S.-H. Yu, Pumping through porous hydrophobic/oleophilic materials: an alternative technology for oil spill remediation, Angew. Chem. 126 (2014) 3686–3690.
[24] Z. Wang, Y. Xu, Y. Liu, L. Shao, A novel mussel-inspired strategy toward superhydrophobic surfaces for self-driven crude oil spill cleanup, J. Mater. Chem. A 3 (2015) 12171–12178.
[25] T. Kim, J.S. Lee, G. Lee, D.K. Seo, Y. Baek, J. Yoon, S.M. Oh, T.J. Kang, H.H. Lee, Y.H. Kim, Autonomous graphene vessel for suctioning and storing liquid body of spilled oil, Sci. Rep. 6 (2016) 22339.
[26] D. Deng, D.P. Prendergast, J. MacFarlane, R. Bagatin, F. Stellacci, P.M. Gschwend, Hydrophobic meshes for oil spill recovery devices, ACS Appl. Mater. Interfaces 5 (2013) 774–781.
[27] Q. Zhu, Q. Pan, Mussel-Inspired direct immobilization of nanoparticles and application for oil–water separation, ACS Nano 8 (2014) 1402–1409.
[28] D.H. Kim, M.C. Jung, S.-H. Cho, S.H. Kim, H.-Y. Kim, H.J. Lee, K.H. Oh, M.-W. Moon, UV-responsive nano-sponge for oil absorption and desorption, Sci. Rep. 5 (2015) 12908.
[29] J. Hu, T. Zhao, W. Geng, Y. Lu, X.F. Zhao, Y.Z. Li, Y.Q. Tang, J.W. Liu, L.Y. Wang, C. Janiak, X.Y. Yang, B.L. Su, Synthesis of hydrophobic and hydrophilic TiO_2 nanofluids for transformable surface wettability and photoactive coating, Chem. Commun. 55 (2019) 9275–9278.
[30] J. Li, Y. Chen, J. Gao, Z. Zuo, Y. Li, H. Liu, Y. Li, Graphdiyne sponge for direct collection of oils from water, ACS Appl. Mater. Interfaces 11 (2019) 2591–2598.
[31] J.-Y. Hong, E.-H. Sohn, S. Park, H.S. Park, Highly-efficient and recyclable oil absorbing performance of functionalized graphene aerogel, Chem. Eng. J. (Lausanne) 269 (2015) 229–235.
[32] J. Ge, L.-A. Shi, Y.-C. Wang, H.-Y. Zhao, H.-B. Yao, Y.-B. Zhu, Y. Zhang, H.-W. Zhu, H.-A. Wu, S.-H. Yu, Joule-heated graphene-wrapped sponge enables fast clean-up of viscous crude-oil spill, Nat. Nanotechnol. 12 (2017) 434.
[33] A.P. Gaur, S. Sahoo, M. Ahmadi, S.P. Dash, M.J. Guinel, R.S. Katiyar, Surface energy engineering for tunable wettability through controlled synthesis of MoS_2, Nano Lett. 14 (2014) 4314–4321.
[34] A. Kozbial, X. Gong, H. Liu, L. Li, Understanding the intrinsic water wettability of molybdenum disulfide (MoS_2), Langmuir 31 (2015) 8429–8435.
[35] Z. Yu, F.F. Yun, Y. Wang, L. Yao, S. Dou, K. Liu, L. Jiang, X. Wang, Desert beetle-inspired superwettable patterned surfaces for water harvesting, Small 13 (2017) 1701403.
[36] X. Gao, X. Wang, X. Ouyang, C. Wen, Flexible superhydrophobic and superoleophilic MoS_2 sponge for highly efficient oil-water separation, Sci. Rep. 6 (2016) 27207.
[37] M. Acerce, D. Voiry, M. Chhowalla, Metallic 1T phase MoS_2 nanosheets as supercapacitor electrode materials, Nat. Nanotechnol. 10 (2015) 313.
[38] S.-J. Choi, T.-H. Kwon, H. Im, D.-I. Moon, D.J. Baek, M.-L. Seol, J.P. Duarte, Y.-K. Choi, A polydimethylsiloxane (PDMS) sponge for the selective absorption of oil from water, ACS Appl. Mater. Interfaces 3 (2011) 4552–4556.
[39] D. Zhu, S. Handschuh-Wang, X. Zhou, Recent progress in fabrication and application of polydimethylsiloxane sponges, J. Mater. Chem. A 5 (2017) 16467–16497.
[40] D. Choi, J. Yoo, S.M. Park, D.S. Kim, Facile and cost-effective fabrication of

patternable superhydrophobic surfaces via salt dissolution assisted etching, Appl. Surf. Sci. 393 (2017) 449–456.
[41] J.-W. Han, B. Kim, J. Li, M. Meyyappan, Flexible, compressible, hydrophobic, floatable, and conductive carbon nanotube-polymer sponge, Appl. Phys. Lett. 102 (2013) 051903.
[42] C. Yu, C. Yu, L. Cui, Z. Song, X. Zhao, Y. Ma, L. Jiang, Facile preparation of the porous PDMS oil-absorbent for oil/water separation, Adv. Mater. Interfaces 4 (2017) 1600862.
[43] X. He, X. Mu, Q. Wen, Z. Wen, J. Yang, C. Hu, H. Shi, Flexible and transparent triboelectric nanogenerator based on high performance well-ordered porous PDMS dielectric film, Nano Res 9 (2016) 3714–3724.
[44] K.Y. Lee, J. Chun, J.-H. Lee, K.N. Kim, N.-R. Kang, J.-Y. Kim, M.H. Kim, K.-S. Shin, M.K. Gupta, J.M. Baik, S.-W. Kim, Hydrophobic sponge structure-based triboelectric nanogenerator, Adv. Mater. 26 (2014) 5037–5042.
[45] S. Lim, B. Cho, J. Bae, A.R. Kim, K.H. Lee, S.H. Kim, M.G. Hahm, J. Nam, Electrohydrodynamic printing for scalable MoS_2 flake coating: application to gas sensing device, Nanotechnology 27 (2016) 435501.
[46] J.N. Coleman, M. Lotya, A. O'Neill, S.D. Bergin, P.J. King, U. Khan, K. Young, A. Gaucher, S. De, R.J. Smith, I.V. Shvets, S.K. Arora, G. Stanton, H.-Y. Kim, K. Lee, G.T. Kim, G.S. Duesberg, T. Hallam, J.J. Boland, J.J. Wang, J.F. Donegan, J.C. Grunlan, G. Moriarty, A. Shmeliov, R.J. Nicholls, J.M. Perkins, E.M. Grieveson, K. Theuwissen, D.W. McComb, P.D. Nellist, V. Nicolosi, Two-dimensional nanosheets produced by liquid exfoliation of layered materials, Science 331 (2011) 568–571.
[47] A.E. Ismail, G.S. Grest, D.R. Heine, M.J. Stevens, M. Tsige, Interfacial structure and dynamics of siloxane Systems: PDMS – Vapor and PDMS – Water, Macromolecules 42 (2009) 3186–3194.
[48] D. Quere, Wetting and roughness, Annu. Rev. Mater. Res. 38 (2008) 71–99.
[49] L.M. Diamante, T. Lan, Absolute viscosities of vegetable oils at different temperatures and shear rate range of 64.5 to 4835 s^{-1}, J. Food Process. 2014 (2014) 1–6.
[50] X. Gui, H. Li, K. Wang, J. Wei, Y. Jia, Z. Li, L. Fan, A. Cao, H. Zhu, D. Wu, Recyclable carbon nanotube sponges for oil absorption, Acta Mater. 59 (2011) 4798–4804.
[51] Q. Zhu, Q. Pan, F. Liu, Facile removal and collection of oils from water surfaces through superhydrophobic and superoleophilic sponges, J. Phys. Chem. C 115 (2011) 17464–17470.
[52] D.D. Nguyen, N.-H. Tai, S.-B. Lee, W.-S. Kuo, Superhydrophobic and superoleophilic properties of graphene-based sponges fabricated using a facile dip coating method, Energy Environ. Sci. 5 (2012) 7908–7912.
[53] N. Bhardwaj, A.N. Bhaskarwar, A review on sorbent devices for oil-spill control, Environ. Pollut. 243 (2018) 1758–1771.
[54] S. Kim, H.J. Hwang, H. Cho, D. Choi, W. Hwang, Repeatable replication method with liquid infiltration to fabricate robust, flexible, and transparent, anti-reflective superhydrophobic polymer films on a large scale, Chem. Eng. J. 350 (2018) 225–232.
[55] R.M. Charin, G.M.T. Chaves, K. Kashefi, R.P. Alves, F.W. Tavares, M. Nele, Crude oil electrical conductivity measurements at high temperatures: introduction of apparatus and methodology, Energy Fuels 31 (2017) 3669–3674.